High-latitude salinity effects and interhemispheric thermohaline circulations

Frank Bryan*

Geophysical Fluid Dynamics Program, Princeton University, Princeton, New Jersey 08542, USA

A general circulation model for the ocean is used to investigate the interaction between the global-scale thermohaline circulation and the salinity distribution. It is shown that an equatorially asymmetric circulation can be maintained even under equatorially symmetric basin geometry and surface forcing. Multiple equilibrium solutions are obtained for the same forcing by perturbing the high-latitude salinity field in an otherwise equatorially symmetric initial condition. The timescale of the transition from the symmetric circulation to an asymmetric circulation depends critically on the sign of the initial salinity perturbation.

THE thermohaline circulation is that part of the total ocean circulation which is driven by fluxes of heat and fresh water through the sea surface, and is often pictured as an overturning of the oceans in the meridional-vertical plane. In contrast to the quasi-horizontal wind-driven gyres, which are confined to limited ranges of latitude, the thermohaline-driven overturning cells are global in scale, and there is a high degree of asymmetry in the sense and intensity of the circulation between basins. The interhemispheric and inter-basin water mass exchanges associated with the thermohaline circulation have an important influence on the distribution of properties in the deep ocean[1], and on global-scale heat and fresh-water transports[2]. Analyses of palaeoclimatic data[3,4] suggest that the strength and pattern of the thermohaline circulation have changed significantly between glacial and interglacial periods, and several authors[4–6] have proposed (largely qualitative) theories for glacial/interglacial climate variability in which the thermohaline circulation plays a central role. A common element of each of these theories is the interaction between the thermohaline circulation and the salinity distribution. The study described here attempts to model these interactions in a quantitative, dynamical framework, using a three-dimensional general circulation model of the ocean.

Role of salinity

Our present understanding of ocean dynamics is insufficient to explain the differences in the sense or magnitude of the thermohaline circulation between basins, or how they might change with time. Several studies[7,8], however, have pointed to the importance of the high-latitude salinity field in controlling the location of deep water formation and in driving interhemispheric circulations. Deep water formation occurs in only a few localized regions, primarily in the high-latitude North Atlantic and around the Antarctic continent[9]. There is a conspicuous lack of deep water formation in the North Pacific. It has long been recognized that this is due to the low surface salinities in the sub-polar North Pacific, which prevent surface water cooled even to the freezing point from overturning with the more saline deep waters[10]. A related, and in fact inseparable problem is to explain what maintains the salinity difference between ocean basins[7].

Relatively few ocean modelling studies have included salinity as a prognostic variable. There are a number of differences between the effects of temperature and salinity, however, which are important in the context of the large-scale thermohaline circulation. First, the equation of state of sea water is nonlinear, so that the relative importance of temperature and salinity variations in the buoyancy field depend on the temperature and salinity themselves. Temperature variations dominate the buoyancy distribution at high temperatures and salinity variations dominate at low temperatures (and hence at high latitudes, where deep water forms). Secondly, there is an important difference between the nature of their respective surface forcings. There is a strong feedback between sea surface temperature (SST) and its atmospheric forcing through the temperature dependence of latent and sensible heat fluxes and long-wave radiation. Surface salinity, on the other hand, has negligible direct effects on evaporation and precipitation, which provide its surface forcing. Many of the ocean modelling studies which did include salinity neglected to take this latter difference into account. In addition, it is common in ocean[11,12] and climate[13] modelling to use highly simplified continent–ocean geometries and to impose a symmetry condition at the Equator, to save computational resources. An equatorial symmetry condition, however, does not allow interhemispheric thermohaline circulations, which are a real and important part of the climate system.

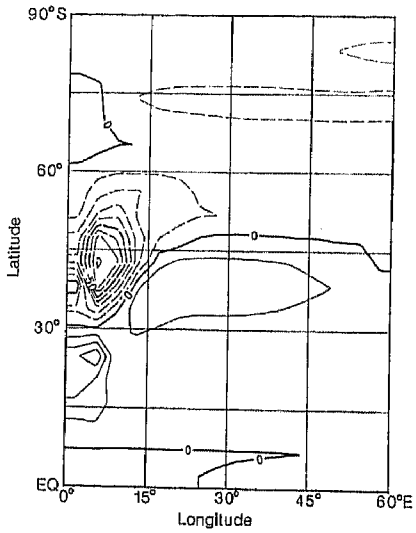

Fig. 1 Virtual surface salt flux distribution used for all experiments, mg m^{-2} s^{-1}.

The model and surface forcing

The general circulation model is based on a finite difference formulation of the primitive equations of motion[14,15]. It includes both temperature and salinity as prognostic state variables, and uses a polynomial approximation of the equation of state[16]. The basin geometry is a 60°-wide sector of the sphere extending from pole to pole, with a flat bottom at 5 km depth. The horizontal resolution is 3.75° longitude × 4.5° latitude, with 12 levels in the

* Present address: National Center for Atmospheric Research, Boulder, Colorado 80307, USA

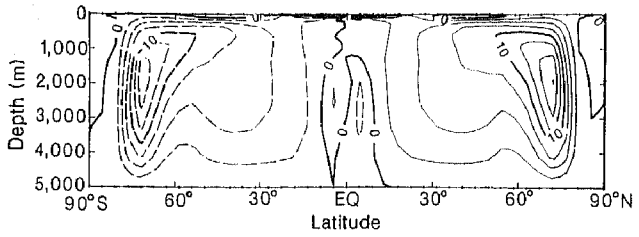

Fig. 2 Stream-function for the zonally integrated meridional overturning circulation for experiment 1 at the end of the integration. Positive values indicate a clockwise circulation; contour interval, 2.5×10^6 m^3 s^{-1}.

vertical dimension. The choice of model parameters is such as to suppress any time variability arising from hydrodynamic instabilities. Sea ice is not taken into account. A complete description of the model physics and numerical implementation are provided elsewhere[11,15].

A wind stress is applied, which approximates the observed zonal mean stress. The surface heat flux is parameterized by a newtonian cooling law[17], in which the flux is linearly proportional to the difference between the predicted SST and a prescribed zonal mean equilibrium temperature (taken as the observed[18] zonal mean SST, averaged over all oceans and both hemispheres). This type of boundary condition can also be thought of as restoring the model SST towards the prescribed distribution on a timescale taken here as 25 days. The salinity surface boundary condition is a fixed virtual salt flux (to represent evaporation, precipitation and runoff). Thus, as discussed above, whereas there is a feedback between the surface heat flux and surface temperature, the surface salt flux is independent of surface salinity. All boundary conditions are symmetric with respect to the Equator.

The specification of the wind and equilibrium temperature distributions is straightforward; however, specifying the virtual salt flux requires more careful consideration. Neither evaporation nor precipitation is well measured over the ocean, and it is not clear how to specify their distributions for the idealized geometry used here. In order to conserve computational resources, I have used the results from a previous experiment[11] with a single-hemisphere version of the model, which was forced with a newtonian-cooling-type condition on salinity as well as on temperature. From the equilibrium solution of this experiment the surface salt flux required to maintain the predicted surface salinity distribution could be computed diagnostically, and is shown in Fig. 1. Note that while the equilibrium salinity profile used in the newtonian-cooling-type condition is zonally symmetric, the implied flux is a function of both latitude and longitude. The magnitude of the flux is largest where transport processes within the ocean (such as advection in the western boundary current) drive the surface salinity furthest from the prescribed values. This salt flux distribution, reflected across the Equator, was then used for all the experiments in the present study.

Initialization

Four experiments are described below, which differ only in their initial conditions. The solution from which the surface salt flux distribution was diagnosed was used as a basic initial condition; however, some problems were experienced in using this initial condition with flux boundary conditions. Had this solution been in exact equilibrium with the surface forcing and perfectly steady, then we would not expect further evolution of the solution after the switch in boundary condition type. For both one- and two-hemisphere versions of the model this was found not to be the case[11]. When the flux boundary condition was applied to salinity, the pre-existing polar halocline became stronger and spread equatorward. As the halocline spread, the meridional circulation collapsed. This behaviour is not completely understood, but was traced to intermittency in convection near the edge of the halocline. It was found that by adding positive (0.5–2.0‰) salinity perturbations to the high-latitude surface layer (the upper 50 m) of the basic initial condition (effectively moving the halocline away from the main deep water formation region) this behaviour could be avoided. The resulting steady circulation did not differ greatly from that in the unperturbed basic initial condition.

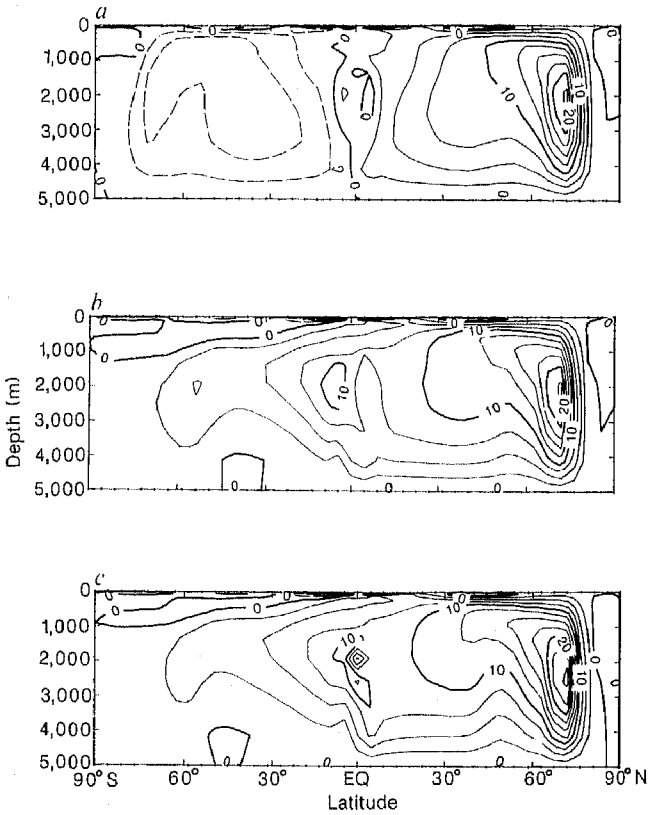

Fig. 3 Stream-function for the zonally integrated meridional overturning circulation for experiment 2 at years 15 (*a*), 44 (*b*) and 68 (*c*). Positive values indicate a clockwise circulation; contour interval, 2.5×10^6 m^3 s^{-1}.

Symmetric circulation

Based on his analysis of a simple hydraulic loop model, Rooth[8] suggested that an initially equatorially symmetric circulation, forced as described above, would be unstable to infinitesimal asymmetric perturbations and would develop into a pole-to-pole circulation. In order to test this, a control case was initialized with a symmetric state (the basic initial condition was modified by adding positive salinity perturbations of 2‰ to the surface layer poleward of 45° latitude in both hemispheres to prevent the initial halocline instability described above). The model was then integrated forward for >1,300 yr. Although there were some very slight differences in the circulation between the two hemispheres, the solution remained essentially equatorially symmetric for the length of the integration. Figure 2 shows the stream-function for the zonally integrated meridional overturning. The final solution was close to equilibrium, as measured by deep water temperature tendencies and net surface heat fluxes. This implies that the three-dimensional, equatorially symmetric circulation is stable to very small perturbations (arising from numerical round-off error), or that the growth rate of any such instability is extremely small.

Asymmetric circulations

The above results do not rule out the possibility of finite-amplitude perturbations exciting a pole-to-pole mode. The

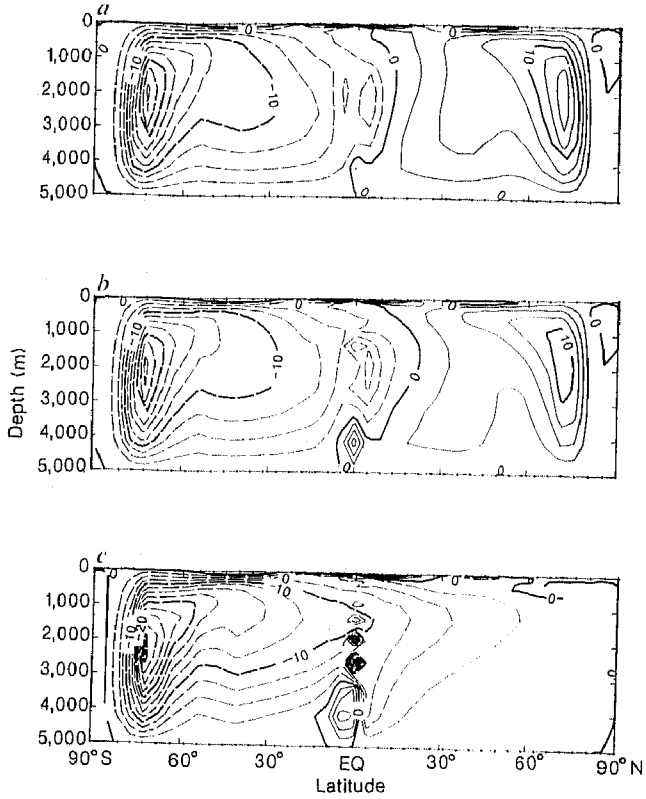

Fig. 4 Stream-function for the zonally integrated meridional overturning circulation for experiment 3 at years 342 (*a*), 411 (*b*) and 534 (*c*). Positive values indicate a clockwise circulation; contour interval, 2.5×10^6 m^3 s^{-1}.

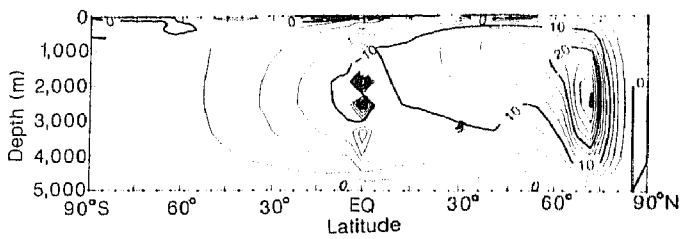

Fig. 5 Stream-function for the zonally integrated meridional overturning circulation for experiment 4 at the end of the integration. Positive values indicate a clockwise circulation; contour interval, 2.5×10^6 m^3 s^{-1}.

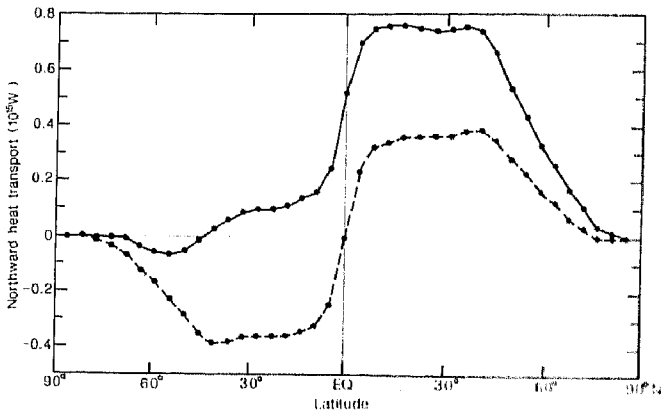

Fig. 6 Northward heat transport for experiment 4 (solid line) at the end of the integration, and for the symmetric solution obtained with newtonian-cooling-type boundary conditions on both temperature and salinity (dashed line).

second experiment was initialized with an intermediate state of the control case (a nearly converged symmetric circulation), with a negative salinity anomaly of 1‰ added to the surface layer poleward of 45° in the Southern Hemisphere. This experiment was meant to represent the response to a pulse of freshwater input to the surface layer, as might occur during deglaciation. The freshening of the surface layer caused deep convection in the Southern Hemisphere to be interrupted, and hence the residence time of water parcels in the surface layer to increase. With a fixed flux boundary condition, the degree to which the surface salinities are modified depends on the residence time of a parcel at the surface as well as the magnitude of the flux. Thus, cessation of deep water formation (in a region of net precipitation over evaporation) led to further freshening of the surface layers. This is a positive feedback on the initial anomaly, and is part of the mechanism described by Warren[7] to account for the lack of deep water formation in the North Pacific. In the absence of active deep water formation, the thermohaline circulation in the Southern Hemisphere collapsed. The decreased advection of high-salinity surface water to high southern latitudes by the thermohaline circulation led to a further decrease in the salinity there. The interhemispheric salinity contrast established in this way provided the buoyancy forces needed to drive an interhemispheric circulation, and a pole-to-pole mode was established within ~50 yr (Fig. 3).

The third experiment was initialized with the same solution as the previous case, except that a 2‰ positive salinity anomaly was added to the Southern Hemisphere polar region. The positive anomaly was rapidly mixed vertically by convection, and led to a slight intensification of the meridional circulation in the Southern Hemisphere. As the circulation intensified, it spread slightly across the Equator (Fig. 4*a*,*b*). The cross-equatorial circulation caused high-salinity surface water to flow into the Southern Hemisphere at the surface, and low-salinity water to flow out at depth. The net advection of salinity into the Southern Hemisphere is, again, a positive feedback on the initial anomaly. In contrast to the feedback seen in the previous experiment, which was a local interaction between deep convection and vertical salinity differences, the feedback in this case is a global interaction between horizontal salinity differences and the strength of the large-scale circulation. This is the mechanism proposed by Rooth[8] to provide the buoyancy force to drive the interhemispheric circulation. A pole-to-pole circulation was eventually established (Fig. 4*c*), but on a much longer timescale than in the case of a negative salinity anomaly.

The final experiment was initialized with the basic initial condition, modified by a positive salinity anomaly added to the Northern Hemisphere polar region. In this case the spread of the Southern Hemisphere polar halocline in the unmodified basic initial condition triggered the pole-to-pole circulation by the same mechanism as in the second experiment. This case was run for >1,200 yrs until a new equilibrium was fully achieved, so that the differences in the climatic properties of the symmetric and asymmetric solutions could be examined. The meridional circulation (Fig. 5) shows that approximately the same amount of deep water forms as in the symmetric case, but the sinking branch is confined to the Northern Hemisphere. The small overturning cells of alternating sign on the Equator (also evident in Fig. 4) are due to inertial instability of the cross-equatorial flow. This type of instability is not scale-selective, and hence appears at the smallest realizable scales in the model (2 grid intervals). Although the instability mechanism is physical, it is not properly resolved by the model and should be parameterized in some way in future studies. The surface salinities in the Southern Hemisphere polar region remain very low, and there is a salinity contrast of ~3‰ between the high latitudes of the two hemispheres. The absence of convection results in very slight surface cooling in the high-latitude Southern Hemisphere.

Thus, the poleward heat transport is dramatically different from that in the symmetric case (Fig. 6). There is equatorward transport over much of the Southern Hemisphere and a cross-equatorial heat flux of the same magnitude as the maximum transport in the symmetric case. Oceanic heat transports of this magnitude could lead to a significant difference between the climates of the two hemispheres.

Discussion

These experiments confirm the hypothesis of Rooth[8] that interhemispheric pole-to-pole circulations can be maintained even under symmetric forcing, but a finite-amplitude salinity anomaly is required to cause an equatorially symmetric circulation to develop into an asymmetric one. At equilibrium, the contrast in salinity between high-latitude regions provides the buoyancy force needed to drive the interhemispheric circulation. The salinity contrast is in turn maintained by the asymmetric thermohaline circulation. The system described here has at least three equilibrium solutions for the same forcing: an equatorially symmetric circulation and two mirror-image pole-to-pole circulations. The response to a negative surface salinity perturbation is rapid and leads to a transition from a symmetric to an asymmetric circulation on a timescale of <100 yr. The response to a positive salinity anomaly, on the other hand, is very slow, leading to a transition from a symmetric circulation to an asymmetric circulation over many hundreds of years. The pulse-like nature of the perturbations used in this study prevent these results from being directly compared to the oceanic response to salinity changes caused by glacial buildup or collapse, which occur over relatively long timescales. Nevertheless, an understanding of the mechanisms which were identified in these experiments will be useful in interpreting the changes in ocean circulation that occur during these climatic transitions.

These experiments provide a first look at the complicated behaviour which can result from the interaction of the salinity distribution and the thermohaline circulation. They were designed to illustrate only processes operating within the ocean, and many other processes which are important in the climate system have been neglected. In particular, one would like to know whether multiple equilibria may still exist for asymmetric surface forcing or basin geometry (as occur in the real world), and to determine the processes involved in the transition from one asymmetric state to another (rather than from the symmetric state to an asymmetric state, as modelled here). Also, the large changes in sea surface temperature between the different solutions would be expected to cause changes in the atmospheric forcing, especially in the evaporative fluxes, which were held constant in these experiments. Future studies should investigate the robustness of these results with respect to changes in basin geometry and surface forcing, and the inclusion of neglected features, such as sea ice and interactive atmospheric circulations. The results of such a study should help to answer the question posed by Broecker *et al.*[4]: "Does the ocean-atmosphere system have more than one stable mode of operation?".

I thank Drs Jorge Sarmiento, Claes Rooth, Kirk Bryan and Syukuro Manabe for their advice and support during this study. This work was completed while I was a graduate student in the Geophysical Fluid Dynamics Program at Princeton University, and supported through a research assistantship under NSF grant ATM8106800.

Received 19 May; accepted 11 August 1986.

1. Reid, J. L. & Lynn, R. J. *Deep Sea Res.* **18**, 1063–1088 (1971).
2. Bryan, K. *A. Rev. Earth planet. Sci.* **10**, 15–38 (1982).
3. Boyle, E. A. & Keigwin, L. D. *Science* **218**, 784–787 (1982).
4. Broecker, W. S., Peteet, D. M. & Rind, D. *Nature* **315**, 21–26 (1985).
5. Weyl, P. K. *Met. Monogr.* **8**, 37–62 (1968).
6. Walin, G., *Palaeogeogr. Palaeoclimatol. Palaeoecol.* **50**, 323–332 (1985).
7. Warren, B. A. *J. mar. Res.* **41**, 327–347 (1983).
8. Rooth, C. *Prog. Oceanogr.* **11**, 131–149 (1982).
9. Killworth, P. D. *Rev. Geophys. Space Phys.* **21**, 1–26 (1983).
10. Reid, J. L. *Intermediate Waters of the North Pacific Ocean* (Johns Hopkins University Press, Baltimore, 1965).
11. Bryan, F. Thesis, Princeton Univ. (1986).
12. Cox, M. D. & Bryan, K. *J. phys. Oceanogr.* **14**, 674–687 (1984).
13. Bryan, K., Komro, F. G., Manabe, S. & Spelman, M. J. *Science* **215**, 56–58 (1982).
14. Bryan, K. *J. comput. Phys.* **4**, 347–376 (1969).
15. Cox, M. D. *Geophys. Fluid Dyn. Lab. Ocean Gp tech. Rep.* No. 1 (Princeton University, 1984).
16. Bryan, K. & Cox, M. D. *J. phys. Oceanogr.* **2**, 510–514 (1972).
17. Haney, R. L. *J. phys. Oceanogr.* **1**, 241–248 (1971).
18. Levitus, S. *Climatological Atlas of the World Ocean* (Natn. Oceans Atmos. Adm. prof. Pap. No. 13) (US Government Printing Office, Washington, 1982).

Novel subunit–subunit interactions in the structure of glutamine synthetase

Robert J. Almassy*, Cheryl A. Janson*, R. Hamlin†, N-H. Xuong† & David Eisenberg*

* Molecular Biology Institute and Department of Chemistry and Biochemistry, University of California at Los Angeles, Los Angeles, California 90024, USA

† Departments of Biology, Chemistry and Physics, University of California at San Diego, La Jolla, California 92093, USA

We present an atomic model for glutamine synthetase, an enzyme of central importance in bacterial nitrogen metabolism, from X-ray crystallography. The 12 identical subunits are arranged as the carbon atoms in two face-to-face benzene rings, with unusual subunit contacts. Our model, which places the active sites at the subunit interfaces, suggests a mechanism for the main functional role of glutamine synthetase: how the enzyme regulates the rate of synthesis of glutamine in response to covalent modification and feedback inhibition.

THE large size (relative molecular mass, $M_r = 12 \times 51{,}628$) and complex pattern of regulation of bacterial glutamine synthetase (GS) stem from its central role in cellular nitrogen metabolism[1–3]. It catalyses the condensation of ammonia with glutamate to yield glutamine, which in turn is a source of nitrogen in the biosynthesis of many metabolites, eight of which act as feedback inhibitors on GS (Fig. 1). GS is also regulated by covalent odification[4]; when glutamine is abundant, tyrosyl residue 397 is adenylylated, which increases the sensitivity of GS to most feedback inhibitors. During the course of its normal function at least 15 known substrates, inhibitors, metals and proteins bind to GS. We seek to understand how these 15 ligands are linked in the control of synthesis of glutamine.

Eighteen years ago, structural studies by electron microscopy revealed that the 12 polypeptide chains of bacterial GS are arranged in two rings of six[5], with 622 point-group symmetry.